



## City Research Online

### City, University of London Institutional Repository

---

**Citation:** Colyer, B., Bak, M., Basanta, D. & Noble, R. (2024). A seven-step guide to spatial, agent-based modelling of tumour evolution. *Evolutionary Applications: evolutionary approaches to environmental, biomedical and socio-economic issues*, 17(5), doi: 10.1111/eva.13687

This is the accepted version of the paper.

This version of the publication may differ from the final published version.

---

**Permanent repository link:** <https://openaccess.city.ac.uk/id/eprint/32738/>

**Link to published version:** <https://doi.org/10.1111/eva.13687>

**Copyright:** City Research Online aims to make research outputs of City, University of London available to a wider audience. Copyright and Moral Rights remain with the author(s) and/or copyright holders. URLs from City Research Online may be freely distributed and linked to.

**Reuse:** Copies of full items can be used for personal research or study, educational, or not-for-profit purposes without prior permission or charge. Provided that the authors, title and full bibliographic details are credited, a hyperlink and/or URL is given for the original metadata page and the content is not changed in any way.

---

City Research Online:

<http://openaccess.city.ac.uk/>

[publications@city.ac.uk](mailto:publications@city.ac.uk)

---







## A seven-step guide to spatial, agent-based modelling of tumour evolution

Journal:	<i>Evolutionary Applications</i>
Manuscript ID	EVA-2024-024-RS.R1
Wiley - Manuscript type:	Review
Keywords:	Disease Biology, Evolutionary Medicine, Population Genetics - Theoretical, Development and Evolution
Note: The following files were submitted by the author for peer review, but cannot be converted to PDF. You must view these files (e.g. movies) online.	
main.tex	

---

# A SEVEN-STEP GUIDE TO SPATIAL, AGENT-BASED MODELLING OF TUMOUR EVOLUTION

---

Blair Colyer <sup>1</sup>, Maciej Bak <sup>1</sup>, David Basanta <sup>2</sup>, and Robert Noble\* <sup>1</sup>

<sup>1</sup>Department of Mathematics, City, University of London, London, UK

<sup>2</sup>Department of Integrated Mathematical Oncology, H. Lee Moffitt Cancer Center and Research Institute,  
Tampa, Florida, USA

\*robert.noble@city.ac.uk

## Author Contributions

Robert Noble conceived the idea for the review; Blair Colyer gathered the review material; Blair Colyer and Robert Noble led the writing of the manuscript with contributions from David Basanta and Maciej Bak. All authors contributed critically to the drafts and gave final approval for publication.

## Acknowledgments

We are grateful to Jill Gallaher, Rafael Bravo and Mark Robertson-Tessi for helpful conversations about model implementation, and to Martín López-García and Grant Lythe for alerting us to potential uses of phase-type distributions.

## ABSTRACT

Spatial agent-based models are frequently used to investigate the evolution of solid tumours subject to localised cell-cell interactions and microenvironmental heterogeneity. As spatial genomic, transcriptomic and proteomic technologies gain traction, spatial computational models are predicted to become ever more necessary for making sense of complex clinical and experimental data sets, for predicting clinical outcomes, and for optimising treatment strategies. Here we present a non-technical step by step guide to developing such a model from first principles. Stressing the importance of tailoring the model structure to that of the biological system, we describe methods of increasing complexity, from the basic Eden growth model up to off-lattice simulations with diffusible factors. We examine choices that unavoidably arise in model design, such as implementation, parameterisation, visualisation, and reproducibility. Each topic is illustrated with examples drawn from recent research studies and state of the art modelling platforms. We emphasise the benefits of simpler models that aim to match the complexity of the phenomena of interest, rather than that of the entire biological system. Our guide is aimed at both aspiring modellers and other biologists and oncologists who wish to understand the assumptions and limitations of the models on which major cancer studies now so often depend.

## Introduction

Cancer initiation, progression, and treatment responses are Darwinian evolutionary processes [1, 2] that can be investigated using a wide range of mathematical and computational methods. Examples include evolutionary game theory [3, 4], branching processes [5, 6], and Moran processes [7, 8]. Yet while many tools have yielded important insights into cancer evolution, the study of spatial aspects – especially important in carcinomas, constituting the majority of humans cancers – often necessitates a spatially explicit approach, such as a spatial agent-based model.

An agent-based (or individual-based) model is a computational model of a system made up of autonomous, interacting “agents”. Spatial agent-based models (SABMs) have long been used to study the evolution of spatially structured communities because they can reveal how the processes of selection, drift, and gene flow depend on localised interactions among agents (typically individual organisms) or between agents and their spatially varying environment. As new technologies generate better spatial tumour data, SABMs are proving ever more useful in oncology. Typical applications include understanding tumour development, inferring the effects of driver mutations, and predicting treatment outcomes. For example in recent studies, Aif *et al.* [9] used an SABM to investigate the evolutionary rescue of drug-resistant tumour subclones; Saha *et al.* [10] used an SABM to investigate adaptive cancer therapy; and Bull and Byrne [11] used an SABM to simulate interactions between macrophages and tumour cells.

To support this burgeoning research field, here we present a seven-step guide to designing and implementing spatial agent-based models in which the agents are locally-interacting tumour cells or cell subpopulations. Starting from the

## A seven-step guide to spatial, agent-based modelling of tumour evolution

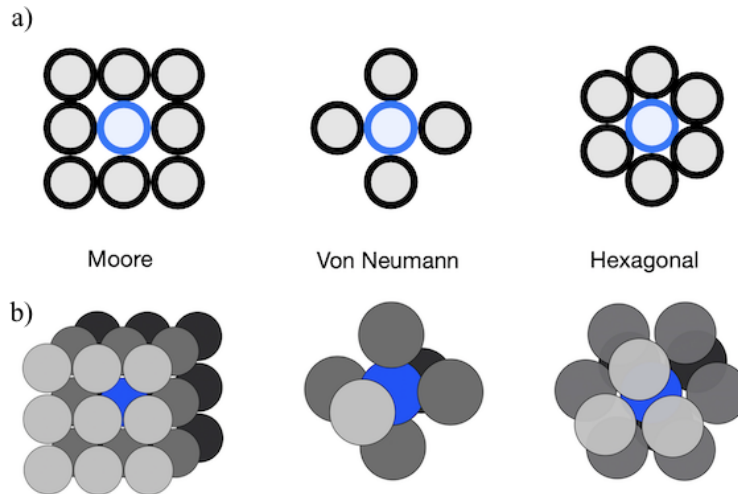


Figure 1: Some common neighbourhoods that govern the update rules for cellular automata and other agent-based models in two dimensions (a) and three dimensions (b). A focal agent (cell) is shown in blue and its neighbourhood sites in grey.

simplest cellular automata, we discuss options for adding greater complexity and biological realism, such as multi-level spatial structure and environmental heterogeneity. Based on our extensive experience of developing and using SABMs [12, 13, 14, 15], we cover practical issues such as event scheduling, visualisation, and how to use SABMs to infer parameter values from experimental or clinical data. Each topic is illustrated with examples from our own demon-warlock modelling framework [14, 12], other state of the art modelling platforms, and studies that have used SABMs in cancer research. Whereas our focus is on tumour evolution, much of our advice applies equally to similar modelling methods used to study bacterial colonies, invasive species, and organismal development. The guide is designed to be accessible for biologists and clinicians without specialist mathematical knowledge.

## 1 Spatial structure

Spatial structure determines the evolutionary balance between selection and drift, the nature of gene flow between subpopulations, and the strength of ecological interactions. When a model fails to accurately represent the spatial structure of a biological system, the model's predictions and inferences for that system may be highly unreliable [12, 16]. It follows that the parameters of spatial structure – such as the size of locally interacting cell communities and the manner of cell dispersal – should be accorded the same importance as evolutionary parameters in model design. Notwithstanding the trade-off between model simplicity and realism, spatial structure parameters should, as far as possible, be derived or inferred from empirical data.

### 1.1 Stochastic cellular automata

Many of the simplest spatial agent-based models are cellular automata. A cellular automaton is a model that plays out on a grid of sites in one or more dimensions. Each site is associated with one of a set of at least two possible states.

Each site also belongs to a subset of sites called a neighbourhood, of which some examples are shown in Figure 1. For example, the von Neumann neighbourhood in two dimensions contains the nearest sites in the cardinal directions (up, down, left and right). A cellular automaton sequentially updates itself according to a set of rules. The update rules for a given site depend on its own current state and the states of the sites in its neighbourhood.

Whereas the update rules of many cellular automata are deterministic [17], probabilistic rules are more appropriate for modelling stochastic processes such as biological evolution. A stochastic cellular automaton is equivalent to a collection of locally interacting Markov chains, which means that each event is chosen according to probabilities that depend only on the current model state, not any of its previous states.

In biological terms, each state corresponds to a type of cancer cell or some other entity (such an immune cell or part of the extracellular matrix). Generally we will assume that the focal agents in our models are cancer cells and we will use the terms “agent” and “cell” interchangeably where appropriate. A cellular automaton permits a cell’s event probabilities (for example, its division, death, and dispersal rates) to depend on the number of neighbouring cells. This allows us to account for crowding or Allee effects, such that birth, death or dispersal rates depend on the local or global population size. Event rates can also vary according to the types of the neighbouring cells, for example to simulate cell competition or immune predation.

Models of asynchronous processes, such as cell division in a tumour, typically use asynchronous updating, meaning that only one or a small number of sites are modified per update [18]. In addition to being more realistic, asynchronous updating is often necessary to prevent conflicts. For instance, if two cells are attempting to divide but only one space is available for the two potential daughter cells then one must take priority.

## 1.2 The Eden growth model

Among the simplest stochastic cellular automata is the Eden growth model. This model is typically implemented on a two- or three-dimensional regular square grid with only two possible states: unoccupied ( $S_0$ ) and occupied ( $S_1$ ). With each iteration, the update rule causes a site in the neighbourhood of an  $S_1$  site to switch from  $S_0$  to  $S_1$ . In this way new  $S_1$  sites (cells) are added to the surface of a cluster. The Eden growth model on an  $n$ -dimensional grid self-organises to resemble an  $n$ -dimensional ball with a non-trivial surface. The growth curve of the  $S_1$  population approaches a polynomial of degree  $n$  [19].

The three most popular options for the Eden growth model update rule can be labelled alphabetically:

- **A**vailable site-focussed: Choose at random an  $S_0$  site in the neighbourhood of an  $S_1$  site, and switch it from  $S_0$  to  $S_1$ .
- **B**ond-focussed: Choose at random an  $S_1$  site with a probability proportional to the number of  $S_0$  sites in its neighbourhood, and then randomly choose an  $S_0$  neighbour and switch it to  $S_1$ .

## A seven-step guide to spatial, agent-based modelling of tumour evolution

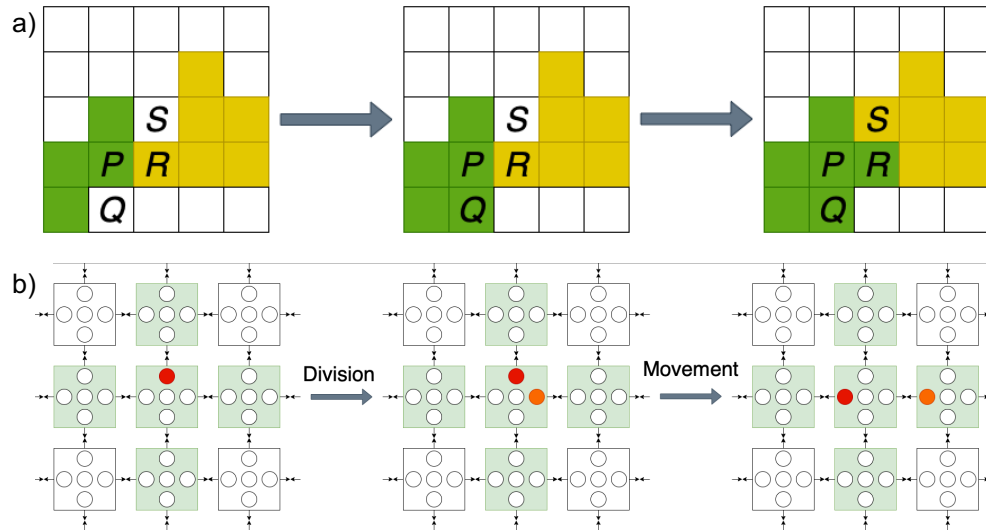


Figure 2: **a)** An illustration of the CPM. Here, two cells, shaded in green and yellow, each occupy multiple sites on a grid. In the leftmost panel, we see the model's initial configuration; in the middle panel, the state of site  $P$  is copied onto site  $Q$ , and the green cell grows; in the rightmost panel, the state of site  $P$  is copied onto site  $R$ , which is initially occupied by the yellow cell, thus deforming the yellow cell and budding it into site  $S$ . **b)** An illustration of the LGCA. Grid sites shaded in green represent those which may influence the focal cell node, shaded in red. The leftmost panel represents the initial configuration; the middle panel shows a cell dividing into free space on its grid site, with the new cell shaded in orange; the rightmost panel demonstrates how cells might move within a grid site or between grid sites: the red cell has changed direction, and the orange cell has moved from one site to another.

- **Cell-focussed:** Choose at random an  $S_1$  site with at least one  $S_0$  site in its neighbourhood, and then randomly choose an  $S_0$  neighbour and switch it to  $S_1$ .

Although these update rules result in similar large-scale patterns, they generate cluster surfaces with different microscopic properties. Indentations in the model surface are more likely to be filled, and spikes are less likely to form, under option C than under option B, and under option B than under option A. Hence option C generates the smoothest surface and option A the roughest [20].

Variants of the Eden growth model have been used to investigate the evolution of paediatric glioma [21], colon cancer [22], hepatocellular carcinoma [23, 24], clear cell renal cell carcinoma [25] and non-small cell lung cancer [26]. Many studies use a variant that includes stochastic cell death. By opening up spaces for cell division, cell deaths increase clonal mixing within the tumour and facilitate selection [23].

### 1.3 Other grid-based stochastic cellular automata

Other stochastic cellular automata can be more appropriate than the Eden growth model for modelling systems in which state changes are not confined to the surface. Spatial branching processes are similar to Eden growth models except that if a dividing cell has no space to divide then it can create space by budding other cells. An intermediate model can be created by stipulating that only nearby cells can be budded, so as to simulate physical constraints on cell division. Chkhaidze *et al.* [27] recently used such a model to investigate how spatially constrained tumour



99 growth alters signatures of clonal selection and genetic drift in cancer genomic data. Good practice is to implement  
100 budding along an approximately straight line between the dividing cell and the nearest empty site. If budding is  
101 instead restricted to the cardinal directions or the cardinal and intercardinal directions then the simulated tumour will  
102 self-organise into an approximate square or octahedron, rather than a more biologically plausible disc or ball.

103 Another option is to allow dividing cells to replace, rather than displace, their neighbours. In the voter model, the  
104 update rule is such that, with a certain probability, a randomly selected site copies the state of a neighbouring site.  
105 Biasses can be introduced by setting unequal copying probabilities, corresponding to differences in cell fitness. Simple  
106 (linear) voter models satisfy a convenient property called coalescing duality, which means that their typical behaviour  
107 can be explained through mathematical analysis [28]. In a pioneering 1972 study, Williams and Bjerknes [29] used a  
108 biased voter model to simulate the spread of skin cancer through the basal epithelial layer.

109 The cellular Potts model (CPM), also known as the Glazier-Graner-Hogeweg model [30, 31], more explicitly simulates  
110 physical interactions among cells and between cells and their microenvironment. The model takes place on a lattice and  
111 each cell is represented by multiple lattice sites (as opposed to only one lattice site, as in previously discussed models),  
112 corresponding to the cell's volume (Figure 2a). Cells are deformable and can adhere to one another or to surrounding  
113 empty sites (which might represent extracellular matrix or growth medium). Hamiltonian mechanics describe the  
114 overall energy of the system depending on adhesion forces and resistance to changes in cell volume. A random lattice  
115 site is chosen at each time step and its state is copied to a random neighbouring site. If the new configuration has lower  
116 energy than the previous configuration then the change is always accepted; otherwise, the probability of accepting  
117 the change depends on the Boltzmann temperature. The CPM has been used in numerous cancer studies, such as  
118 for simulating tumour growth, invasion and evolution [32], or for investigating how cell compressibility, motility and  
119 contact inhibition shape tumour cell clusters [33]. The CompuCell3D modelling environment compucell provides an  
120 efficient, flexible CPM implementation.

121 The biological lattice gas cellular automaton [34] excels instead at modelling cellular movement, and especially col-  
122 lective migration, in a simple, computationally efficient, and physically correct fashion. The model must play out on  
123 a square or hexagonal lattice in 2 dimensions, or a cubic, dodecahedral or icosahedral lattice in 3 dimensions. States  
124 incorporate cell velocities. For instance, consider a 2-dimensional square lattice in which each site contains 5 nodes:  
125 one for each directional velocity and a resting node at the centre (Figure 2b). A cell occupying any one of these nodes  
126 can divide into other nodes on the same site. A cell can also reorient itself by moving between nodes on the same site,  
127 and can move between sites according to its velocity, provided there is space to do so. This model has been used, for  
128 example, to give insights into breast cancer invasion plasticity [35].

#### 129 **1.4 Multi-level spatial structures**

130 An important limitation of all the aforementioned cellular automata is that their uniform spatial structures are in-  
131 consistent with the biology of many tumour types. Various common cancers have glandular structures and grow via

132 individual cells or small cell clusters invading neighbouring tissue [36, 37]. Colorectal adenomas are also glandular  
133 but grow through gland fission [38].

134 Inspired by classical population genetics models [39], a simple, conventional way to account for multi-level spatial  
135 structure in tumours is to assign cells to local subpopulations, called demes, located on a regular grid. Thus each grid  
136 site is allowed to contain not only one but dozens, hundreds, or thousands of cells. The subpopulation size per deme  
137 is prevented from exceeding a certain threshold – known as the deme’s carrying capacity – by decreasing cell division  
138 rates or increasing death rates as the subpopulation size grows.

139 Deme-based models allow for more complicated modes of cell dispersal. As in the voter model, cells can be assigned  
140 some probability of invading neighbouring demes, either individually or in clusters. The dispersal probability can also  
141 be made to depend on the population of the deme being invaded, so that cells disperse more easily in less densely  
142 populated regions near the tumour periphery. Alternatively, each occupied deme can be assigned a probability of  
143 undergoing fission, resulting in some of its cells being moved to an unoccupied neighbouring deme. Depending on  
144 the degree of budding allowed, the deme-level dynamics of the fission model can resemble an Eden growth model (no  
145 budding of demes) or a spatial branching process (unlimited budding). Deme-based models additionally allow for the  
146 explicit simulation of tissue invasion, such that a tumour can grow only via its cells invading demes that are initially  
147 filled with normal cells [12].

## 148 **1.5 Aggregating agents**

149 If the within-deme subpopulations can be assumed to be well-mixed then cells that belong to the same deme and  
150 have the same phenotype and genotype can be modelled collectively, rather than as individual agents. This model  
151 design not only improves computational efficiency but can also facilitate mathematical analysis. For example, when  
152 cells disperse by invading neighbouring demes, the model can be designed so that the dynamics are approximately  
153 equivalent to the well understood spatial Moran process [12]. Cells can be randomly selected within a deme by  
154 sampling from a hypergeometric distribution.

155 Even greater efficiency can be realised by not modelling inter-deme dynamics at all, and simply making the demes  
156 themselves the model agents [40, 41]. Although such coarse-graining enables the simulation of much larger tumours,  
157 it comes at the cost of reduced precision. Care should be taken in translating between mutation rates per cell and  
158 effective mutation rates per deme.

## 159 **1.6 Off-lattice models**

160 Instead of confining agents to a regular grid, we might instead locate them in continuous space. This structure is poten-  
161 tially more realistic but also entails more parameters, more decisions to be made, and typically higher computational  
162 costs [42]. To prevent multiple cells occupying the same space and to maintain tumour integrity, we now must model

163 the movement of cells in response to physical forces such as cellular adhesion and repulsion [43]. We may also choose  
164 to model directed movement under the influence of diffusible factors (haptotaxis).

165 There are several practical ways to prevent cells overlapping in an off-lattice model, depending on how the agents  
166 are implemented. Suppose we have spherical cells, each with fixed radius  $r$ . We can then specify that when, as a  
167 result of cell division or movement, the distance between two cells' centres is less than  $2r$ , both cells will simply be  
168 pushed in opposite directions. Alternatively, to account for cell deformation, we might implement repulsion only when  
169 the distance between cell centres falls below some threshold value smaller than  $2r$  [44]. Some modelling platforms  
170 achieve greater realism and tractability by implementing adhesion and repulsion forces using functions rooted in  
171 physics, which are beyond the scope of this guide (see documentation cited in the appendix).

## 172 **2 Mutation**

173 Having chosen an appropriate spatial structure, we next will decide which cell phenotypes and genotypes to include  
174 in our state space, and how to model mutations between these states. As ever, the goal is to balance model simplicity,  
175 realism, and computational demands.

### 176 **2.1 Defining phenotypes**

177 A good part of the difficulty in designing a useful model stems from the fact that much of the experimental data  
178 gathered by cancer biologists focusses on genetic mutations while the rules that govern the behaviour of the agents in an  
179 SABM assume an understanding of the key cancer phenotypes. The most basic actions a tumour cell might perform at  
180 any given time step are apoptosis/death, proliferation, and motility. These are often considered as simple probabilistic  
181 events and often modelled in an exclusionary manner, so that if a cell is moving then it is neither proliferating nor dying.  
182 The required probabilities can either be taken directly from experimental data (which is often hard to measure *in vivo*  
183 and unrealistic *in vitro*) or calibrated with *in vivo* pre-clinical models.

184 Using hard-coded rules to model the phenotype of a tumor cell, while relatively simple, does not capture the flexibility  
185 shown by biological cells in the mapping between genotype and phenotype. Gerlee and colleagues have instead  
186 proposed capturing some of the complexity of this mapping by embedding neural networks inside each agent, so that  
187 the phenotype emerges in a non-linear way as a result of the agent's state and the different microenvironmental inputs  
188 to which the agent is receptive [45].

### 189 **2.2 Trait evolution versus population (epi)genetic models**

190 Once phenotypes have been defined, the next step is to determine how these phenotypes will change as a result of  
191 mutations. One option is to model mutations as phenotypic switches. Many studies consider models with only two  
192 possible tumour cell states – mutated and unmutated – which differ in fitness [40], degree of drug resistance [46], or  
193 some other trait. Grow-or-go models assume that cells can reversibly switch between predominantly migratory and

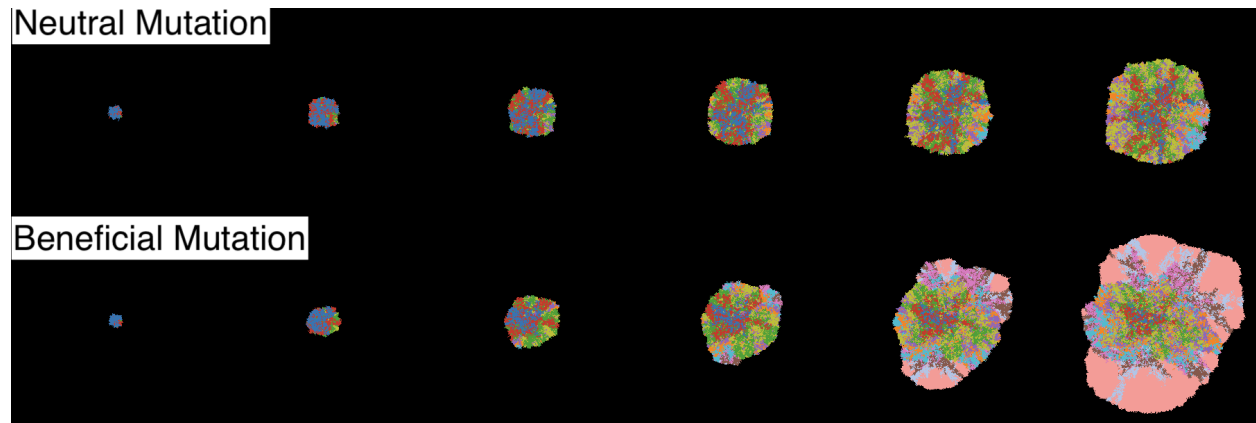


Figure 3: The result of running an Eden growth model with nearly neutral mutations (top) and beneficial mutations (bottom). Model produced in HAL using some in-built examples as a skeleton for the code. [51].

194 predominantly proliferative phenotypes [47]. Other models examine the evolution of continuous traits, such as levels  
 21 of glycolysis and acid production [48].

196 If we are more interested in clonal dynamics then we can explicitly track changes to the (epi)genome. These mutations  
 25 are conventionally assigned to three groups according to how they affect cell fitness: driver mutations (which increase  
 26 cell fitness), passenger mutations (no effect), and deleterious mutations (negative effect). For simplicity, most studies  
 27 assume an infinite sites model [49], such that no two mutations can occur at the same site. Finite sites models must be  
 28 parameterised based on observed mutation frequencies [50].

### 201 2.3 Example: The Eden growth model with mutation

202 We can convert an Eden model into an evolutionary model by implementing mutation. The grid and neighbourhood  
 203 are defined as before but now we have multiple cell states  $S_1, S_2, S_3, \dots$  and mutation rates between each pair of  
 204 distinct cell states. A simple option, assuming infinite sites, is to set all mutation rates to be zero except in the case  
 205 of  $S_i$  to  $S_i + 1$  for all  $i \geq 0$ , so that every  $S_i$  cell has exactly  $i$  mutations. Let us assume that all these mutations are  
 206 drivers and their effects combine multiplicatively, such that each mutation increases the division rate by a factor of  
 207  $1 + s$ , with  $s \geq 0$ . Assume also that mutations occur only at the time of cell division, and the number of new mutations  
 208 per daughter cell is Poisson distributed. We then arrive at a reasonable toy model of spatial tumour evolution that can  
 209 be implemented in not much more than 100 lines of code, as we illustrate with an R script [52]. Figure 3 shows results  
 210 of implementing a similar model in the HAL platform [51].

### 211 2.4 Distributions of fitness effects

212 Modelling the evolution of a quantitative trait, such as cell division or death rate, leads to further design decisions. As  
 213 in our toy model, it can be wiser to draw mutation fitness effects from a probability distribution instead of setting them  
 214 all equal. To see why, consider a model of an expanding tumour that, in the absence of mutation, has radius growth  
 215 rate  $c_0$ , and in which the spread of mutants is not confined to the periphery (for example, a biased voter model).

216 When a new mutant arises within the wildtype population, its long-term fate, in the absence of further mutation, will  
 217 be sensitive to its radius growth rate,  $c_1$ . If  $c_1 < c_0$  then the mutant will remain forever rare; if  $c_1 > c_0$  then the mutant  
 218 is bound to take over the entire tumour; if  $c_1 = c_0$  then the mutant will become relatively more abundant over time  
 219 without ever fully replacing the wildtype. Randomising the fitness effect randomises  $c_1$  and so randomises mutant  
 220 fates. Our demon-warlock framework draws each selection coefficient (relative increase in cell division rate) from an  
 221 exponential distribution.

222 Strictly multiplicative fitness is best avoided in all but the smallest-scale models as it can lead to unrealistically high  
 223 fitness values. This is especially problematic if mutation is implemented at the point of cell division, which creates a  
 224 feedback loop in which lineage fitness grows at an ever increasing rate. A simple solution implemented in our demon-  
 225 warlock framework is diminishing returns epistasis. When the selection coefficient of a driver mutation is  $s$ , instead  
 226 of multiplying the division rate by  $1 + s$ , we instead multiply by  $1 + s(1 - b/b_{max})$ , where  $b$  is the previous division  
 227 rate and  $b_{max}$  is an upper bound.

### 228 3 Event scheduling

229 The next step is to consider how to implement cell events algorithmically. Event scheduling can be the most important  
 230 factor in determining computational efficiency, especially in simpler grid-based models. The optimal choice strikes a  
 231 balance between efficiency, simplicity, and biological realism.

#### 232 3.1 Gillespie's algorithm

233 The Gillespie Stochastic Simulation Algorithm [53] is an especially simple and popular solution to event scheduling.  
 234 Event rates are assumed to depend only on the current state of the model and the time between events is exponentially  
 235 distributed (as in a Poisson process), such that two events cannot occur simultaneously. The steps of the algorithm are  
 236 as follows:

- 237 1. Initialise the system.
- 238 2. Set event rates (birth rates, death rates, dispersal rates, etc.).
- 239 3. Randomly determine the next event such that  $\mathbb{P}(event = E) = rate(E) / \Sigma(rates)$
- 240 4. Implement the chosen event.
- 241 5. Advance the timer by  $\delta t \sim \text{Exp}(1 / \Sigma(rates))$
- 242 6. Repeat from step 2 until a stop condition is reached.

243 This algorithm is more efficient than the event timer approach (see below) and is very easy to implement. In statistical  
 244 terms, the simulated sequence of events corresponds to a trajectory of a set of stochastic differential equations, called  
 245 the master equations. This means we have a good mathematical understanding of how the algorithm behaves.

246 Our toy Eden growth model [52] provides an example implementation of Gillespie’s algorithm. This model further  
247 improves computational efficiency by keeping track of the cells that have space to divide, so that the next dividing cell  
248 can be chosen from among this subset (which in  $n$  dimensions scales with the radius to the power of  $n - 1$ ) rather than  
249 from the entire cell population (which scales with the radius to the power of  $n$ ). The drawback is that cells without  
250 space to divide never undergo mutation, which may be an unjustifiable assumption in a serious research model.

251 Modifications of Gillespie’s algorithm, such as tau leaping [54], are even faster but less accurate. Tau leaping allows  
252 multiple events to occur simultaneously, which may be problematic in a spatial model if the events affect multiple sites  
253 in close proximity (for example, if two cells are chosen to divide into the same empty site). Moreover, tau leaping  
254 improves performance only when the system is dominated by a small number of large, homogeneous subpopulations,  
255 which is typically not the case in SABMs.

### 256 3.2 Gillespie’s algorithm with phase-type distributions

257 A shortcoming of the Gillespie algorithm is that some events, such as cell division, are not true Poisson processes with  
258 exponentially distributed waiting times. In effect, the Gillespie algorithm permits arbitrarily short cell cycles. Some  
259 cells may divide several times while, in the same period, others with identical division rates fail to divide at all.

260 One way to achieve more realistic cell cycle periods without sacrificing very much computational efficiency is to use  
261 a phase-type probability distribution. Whereas an exponential distribution models the time until the next event in a  
262 Poisson process, a phase-type distribution models the time taken for an entire sequence of events, which may occur at  
263 different rates.

264 In practical terms, this entails executing the Gillespie algorithm as above, except that when a cell is selected for  
265 division, it doesn’t necessarily divide immediately, but instead changes its position in the cell cycle. Given a target  
266 probability distribution for cell cycle periods, we can use an algorithm to choose transition rates such that the resulting  
267 phase-type distribution has the same mean, variance, and skew as the target [55]. For example, suppose that all cells  
268 begin in division state 0. When a cell is selected (according to a state-dependent probability), its state is updated from  
269 0 to 1, 1 to 2, or 2 to 3. When a state 3 cell is selected it divides and both progeny are reset to state 0 [56]. The  
270 method’s greater realism comes at the cost of additional memory demands and longer execution time, compared to the  
271 basic Gillespie algorithm.

### 272 3.3 Random sampling with binary trees

273 When we have more than a handful of events to choose from it will be much more efficient to implement event  
274 selection using a binary tree. Suppose, for example, that we have four possible events with rates  $p_1, p_2, p_3$  and  $p_4$ ,  
275 where  $p_1 \leq p_2 \leq p_3 \leq p_4$ . If we store the rate sums  $p_1 + p_2, p_3 + p_4$ , and  $p_1 + p_2 + p_3 + p_4$  then we can choose an  
276 event as follows. First we generate a random number  $r$  from a uniform distribution between 0 and  $p_1 + p_2 + p_3 + p_4$ ,  
277 and we examine whether  $r < p_1 + p_2$ . Supposing  $r$  is greater than  $p_1 + p_2$ , we then test whether it is less than  $p_3$ . If

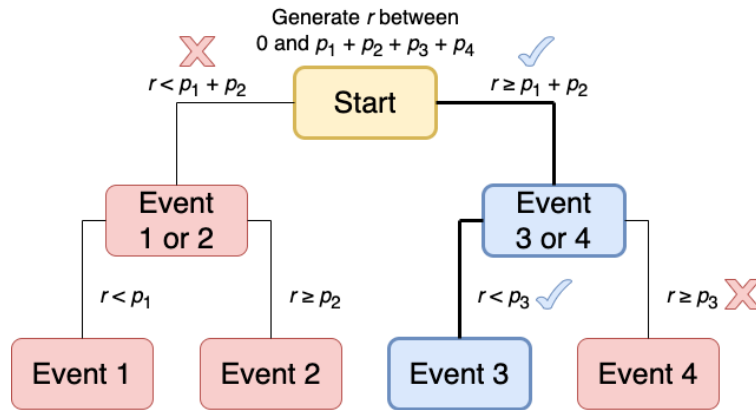


Figure 4: An example of using a binary tree to select an event (Event 3) from four options. Selected nodes are shown in blue.

so then we choose event 3; otherwise event 4. Effectively, we have traversed a binary tree, beginning at the root node associated with the sum of all event rates, and ending at a terminal node associated with a single event (Figure 4).

The binary tree method is efficient because both the number of steps needed to choose an event, and the number of nodes that need updating following a change in an event rate, grow only with the logarithm of the number of possible events. For example, we need only twenty steps to choose between one million possible events. As long as the cell population keeps growing, there is little benefit to pruning nodes and it is easy to ensure that the tree remains balanced. The rate sums together take up only as much computer memory as the individual rates. The main costs are in terms of code development time and code complexity. Binary trees require careful implementation and error checking to ensure that existing nodes are updated and, when required, new nodes are added after each model event. Our demon model implements binary trees and periodically recalculates event rate sums to prevent excessive accumulation of rounding errors.

### 3.4 Cell cycle timers

A less efficient alternative to using phase-type distributions is to draw inter-division times directly from a chosen probability distribution. This approach enables more precise tracking and adjustment of individual cell cycles. An algorithm used in recent studies [48, 46] is as follows:

1. Initially assign every cell  $i$  a countdown timer set to time  $t_i$  drawn from some probability distribution (dependent on the cell's phenotype).
2. Subtract  $\delta t$  from every countdown timer, where  $\delta t \ll t_i$  for all  $i$ .
3. For all cells  $i$ , in random order:
  - A. Implement cell death and dispersal events for  $i$ ;
  - B. If  $i$  is alive, has space to divide, and  $t_i \leq 0$ , then  $i$  divides;
  - C. Assign each new cell a countdown timer, set to some random time dependent on the new cell's phenotype.



1  
2  
3 300 4. Repeat from step two until a stop condition is reached.  
4  
5

6  
7 301 How much this approach reduces computational efficiency will depend on other aspects of the model. It is likely  
8 302 to be much slower than a well implemented Gillespie algorithm when applied to a simple grid-based model, due to  
9  
10 303 the additional burdens of updating every cell (Step 2) and shuffling all the cells (Step 3) at each small time step. In  
11 304 an off-lattice model, where cells move much more frequently than they divide, and where a shuffling algorithm may  
12 305 already be required to randomise the order in which cell positions are updated, the cost of updating cell division state  
13 306 at the same time as position may be negligible.  
14  
15  
16  
17

## 18 307 **4 Microenvironment**

19  
20  
21  
22 308 Whereas many SABM studies focus on the effects of spatial structure and cell-cell interactions, real tumours evolve  
23 309 in a complex microenvironment that varies over space and time. This tumour microenvironment, comprising both  
24 310 molecular elements, such as cytokines, and other (non-cancer) cells, constitutes the cancer ecosystem [57] – a key  
25 311 element of the selection process driving somatic evolution. Given a good rationale and sufficient parameterisation  
26 312 data, we may choose to extend our model by explicitly simulating microenvironmental factors in the form of agents  
27 313 (in the case of immune cells or stromal cells) or diffusible factors (such as oxygen and drugs). Permitting cancer cells  
28 314 to modify their selective environment creates potential for emergent complexity and niche construction [58, 59].  
29  
30  
31  
32  
33  
34

### 35 315 **4.1 Hybrid cellular automata**

36  
37  
38 316 Hybrid cellular automata (or HCA) have been used to model interactions between tumour cells and diffusible factors  
39 317 for more than twenty years. As described in a pioneering 2001 paper by Patel and colleagues [60], these models con-  
40 318 sist of two interdependent components: stochastic cell events, and deterministic reaction-diffusion partial differential  
41 319 equations. The latter component dictates how chemicals or other factors work their way through the system as they  
42 320 are consumed and processed by cells. Local concentrations of diffusible factors contribute to the cell update rules.  
43  
44

45  
46 321 Typically we assume that diffusible factor concentrations rapidly re-equilibriate following changes in the configuration  
47 322 of cells. We can then numerically solve the equations to find the equilibrium concentrations either after every cell event  
48 323 or, trading some accuracy for greater efficiency, after a relatively small number of cell events have occurred. Suitable  
49 324 procedures for solving partial differential equations as initial value problems can readily be found in textbooks and  
50 325 software libraries. These range from simple but inefficient algorithms based on the classical Gauss-Seidel method,  
51 326 which require only a few dozen lines of code [61, 60, 15], to the highly sophisticated BioFVM solver [62], which is  
52 327 specifically optimised for hybrid SABMs. Several SABM platforms include their own methods for solving reaction-  
53 328 diffusion equations in two or three dimensions (see appendix).  
54  
55  
56  
57  
58  
59  
60



## 329 4.2 Types of diffusible factor

330 To add biological realism, we might make cell division and death rates in our model depend on the local oxygen  
331 and glucose concentrations as these factors diffuse through the tumour from the surrounding medium (in very small  
332 tumours and tumour spheroids) or from point sources representing blood vessels (in larger, vascularised tumours). We  
333 might also modify dispersal rates so that cells follow oxygen or glucose gradients. Potential adverse factors include  
334 acid produced through tumour cell metabolism, and drugs that diffuse from blood vessels. Hybrid cellular automata  
335 are especially suitable when the supply of an influential factor is highly variable over space or time, such as in the case  
336 of intermittent drug treatment [63].

## 337 5 Parameterisation and inference

338 Although theoretical models can be valuable for generating hypotheses and providing proof of concept, if we want to  
339 apply an SABM to studying a particular biological system then we must ensure that its influential parameter values are  
340 set appropriately. Parameterisation should ideally be based on clinical or experimental data specific to the biological  
341 system of interest; otherwise values can be estimated from studies of similar systems or theoretical considerations (for  
342 instance, diffusion coefficients approximately correlate with molecular weight). Influential parameters might pertain  
343 to the effects of mutations, drugs, oxygen and glucose; rates of chemical supply, diffusion, consumption and decay;  
344 cell dispersal modes and rates; baseline cell death rates, crowding effects and the size of interacting cell communities.  
345 Since calibrating SABMs is often computationally demanding, high-performance computation may be required to  
346 generate the necessary resources to calibrate them properly.

### 347 5.1 Example: Hybrid cellular automaton for simulating a tumour spheroid

348 Bacevic and Noble *et al* [15] parameterised a HCA to mimic tumour spheroid evolution under drug treatment. In  
349 spheroids the limiting factor for cell survival and proliferation is oxygen. Other diffusible factors such as glucose  
350 were therefore omitted to simplify the model without compromising its usefulness. The oxygen concentration in  
351 the medium and oxygen diffusion rates were drawn from previous studies [64, 65, 66], as were the mathematical  
352 relationships between oxygen consumption rate, cell proliferation rate and local oxygen concentration [67, 68]. The  
353 different maximum proliferation rates of drug-sensitive and resistant cells, reflecting a fitness cost of resistance, were  
354 determined from new monolayer growth assays. Cells with insufficient oxygen supply were assumed to die.

355 Since oxygen effects alone fail to account for the extent of quiescence observed in tumour spheroids, Bacevic and  
356 Noble *et al* implemented crowding effects by permitting cell budding only within a specified radius. New monolayer  
357 growth assays revealed that the relationships between cell proliferation rate, death rate and drug dose could be well  
358 approximated with piecewise linear functions. The drug's impact on proliferation was further assumed to multiply the  
359 oxygen effect, consistent with prior observations [67]. Drug consumption was also modelled using Michaelis-Menten

kinetics, with a diffusion rate chosen according to the drug's molecular weight and an appropriately low consumption rate. Thus parameterized, the SABM accurately predicted the outcomes of new tumour spheroid experiments [15].

## 5.2 Example: Hybrid cellular automaton of the bone ecosystem in cancer

Araujo and colleagues [69] developed a hybrid cellular automaton for which the goal was to capture the ecosystem of the bone. A crude approximation of this ecosystem includes the bone itself, the myeloid-derived cells such as osteoclasts that resorb bone, and the cells derived from mesenchymal stem cells, such as osteoblasts, that deposit new bone. Each of these cell types can be modelled as discrete agents regulated by diffusible factors – such as TGF- $\beta$ , RANK ligand, and other factors embedded in the bone matrix – described by partial differential equations. Parameterisation of the model is facilitated by the fact that non-cancerous cells have more predictable phenotypes, and the model's overall behaviour can be calibrated to ensure it recapitulates bone homeostasis. Araujo and colleagues thus studied how bone metastatic prostate cancer cells could infiltrate the bone ecosystem, take advantage of it, and grow [70]. They also investigated what prostate cancer cells in the primary tumour should be of concern to physicians, and why conventional treatments that fail to disrupt tumour-ecosystem interactions also fail to provide long-term cancer cures in bone metastatic prostate cancer [71].

## 5.3 Parameter inference

Unknown parameter values can be inferred by combining an SABM with a statistical method. This is, in fact, often the main objective of an SABM study. Approximate Bayesian computation is a popular approach that, in its simplest form, infers the value of a parameter  $\theta$  as follows

1. From our data, calculate some summary statistic  $\mu_{data}$ ;
2. Set  $i = 1$ ;
3. Run the model using a candidate parameter value  $\theta_i$  drawn from some prior distribution;
4. Calculate the summary statistic  $\mu_i$  for the model output;
5. If the difference between  $\mu_i$  and  $\mu_{data}$  is less than a predefined tolerance then add  $\theta_i$  to the posterior distribution;
6. Increment  $i$ ;
7. If  $i$  is less than some threshold then repeat from step 3.

Although simple in principle, approximate Bayesian computation requires careful implementation. The accuracy and precision of inferences depend on the choices of prior distributions, summary statistics, and tolerances, as well as the number of iterations. Typically multiple parameter values cannot be precisely derived from prior data or models, in which case each should be assigned a vague (high variance) prior distribution. Tolerance values should be tuned such that neither too many nor too few candidate parameter values are accepted to the posterior distribution. Summary

1  
2  
3 391 statistics should capture features of the system that provide useful information about the parameters of interest. A  
4 392 useful template is a 2010 study [72] in which Sottoriva and Tavaré inferred aspects of stem cell dynamics in the  
5 393 colonic crypt by combining a cellular Potts model with approximate Bayesian computation, using a summary statistic  
6 394 based on methylation patterns.

7  
8  
9 395 An alternative to this approach was recently outlined in [73], in which the authors describe a novel method utilising  
10 396 neural networks to reduce both tumour images and SABM simulations to low-dimensional points. The distance be-  
11 397 tween these points acts as a quantitative measure of how the two differ. This enables direct comparison, and by using  
12 398 parameter fitting algorithms to minimise the distance between the two sets of points, parameters can be estimated  
13 399 directly from the images and the simulations.

## 14 400 **5.4 Sensitivity analysis**

15  
16  
17  
18 401 Whatever the objective, an essential step in any modelling study is to examine, as far as is practical, how the results and  
19 402 conclusions depend on uncertain aspects of the model. A common approach is to run a large number of model variants  
20 403 with different combinations of plausible parameter values. Varying one parameter at a time can provide useful insight  
21 404 into which parameters have the greatest impact on model output, with the shortcoming that non-linear interactions  
22 405 between parameters are often neglected. A more sophisticated approach is to infer a multivariable “metamodel”  
23 406 function – a model of the model – that approximately describes how the model’s parameters determine its outputs.

24  
25 407 Since varying many parameters systematically on a continuous scale is infeasible, sampling methods such as Sobol se-  
26 408 quencing [74] or Latin hypercube sampling [75] can be used to generate a set of near-randomly sampled combinations  
27 409 of parameter values. Both methods were used in a recent SABM study of cancer cell response to ATR-inhibitors [22].  
28 410 A recent introductory review explains specifically how to apply these methods to cancer ABMs [76]. It is important to  
29 411 note that thorough sensitivity analysis involves varying not only parameter values but also mathematical relationships,  
30 412 aspects of spatial structure, and any other influential model components.

## 31 413 **6 Visualisation**

32  
33  
34 414 Having built and parameterised a model, we next require useful ways to visualise its output. Typical methods repre-  
35 415 sent spatial information, multidimensional phenotypic information, or evolutionary dynamics. Representing all these  
36 416 aspects in a single image is generally impossible.

### 37 417 **6.1 Spatial plots**

38  
39  
40  
41 418 A spatial plot represents the state of an SABM at a moment in time. Producing a two-dimensional grid plot of a  
42 419 two-dimensional on-lattice model is straightforward – we simply output the state of each site as a matrix of numbers  
43 420 and input this matrix into a bitmap (or raster) plotting function in R, Python, MATLAB, or similar software, using  
44 421 different colours to represent the different states (Figure 3). Our toy Eden growth model [52] provides an example

## A seven-step guide to spatial, agent-based modelling of tumour evolution

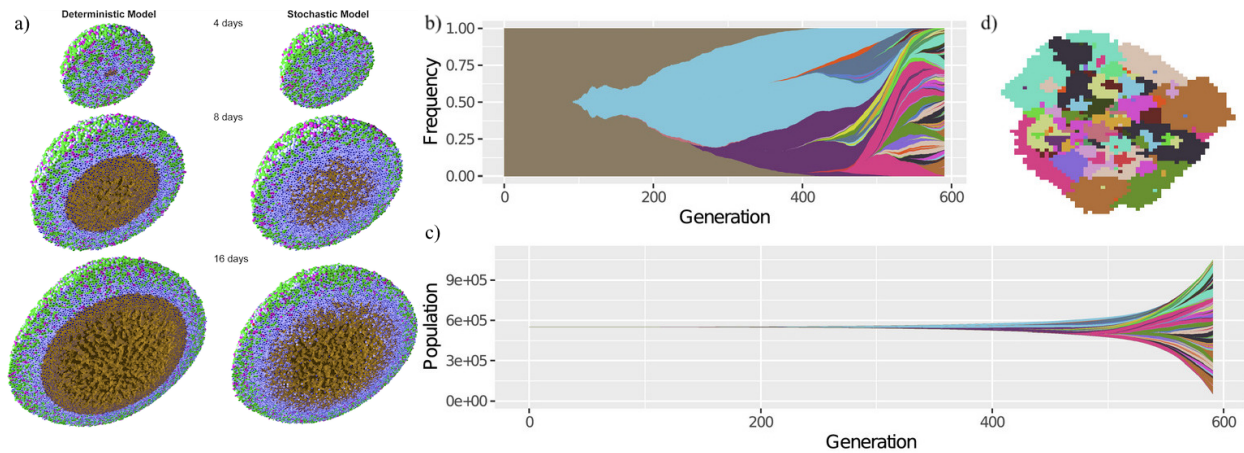


Figure 5: **a)** Plots of a 3D off-lattice ABM, produced in PhysiCell [77], showing a cross-section of model states of a hanging-drop spheroid growth simulation at different time points, using either a deterministic or a stochastic SABM. Cells are coloured according to cell cycle position. Cells in the  $K_1$  cell cycle state are green, post-mitotic  $K_2$  cells are magenta, quiescent cells are pale blue, apoptotic cells are red, and necrotic cells are brown. Cell nuclei are shown in dark blue. **b)** Muller plot showing phylogenies and phenotype frequencies over time. **c)** Fish plot showing phylogenies and phenotype population sizes over time. **d)** 2D grid plot corresponding to same simulation as the Muller and fish plots in previous panels, with the same colour scheme, at the final time point. Plots b and c were produced using the R package *ggmuller* [78]. Image a is reproduced from [77] under the terms of a Creative Commons Attribution License and with the approval of Paul Macklin. Plots b-d are reproduced from [13] under the terms of a Creative Commons Attribution License.

implementation. Diffusible factor concentrations can be shown outside the tumour using a colour gradient and inside the tumour by adjusting brightness [15]. We can apply the same method to off-lattice models by specifying a grid and assigning each grid square a value that summarises the states of all points within the square. Given multi-level spatial structure, we can represent the most abundant state in each deme [12].

Illustrating three-dimensional information is more technically demanding as we need to project the object onto a two-dimensional plane, determine the visible surface, and add shading (as in Figure 5a). Suitable computational methods include rasterisation and ray tracing, which can be performed in R and Python or using dedicated software, such as POV-Ray. Further details can be found in the PhysiCell documentation (see appendix). A much simpler solution is to plot only two-dimensional slices.

## 6.2 Visualising evolutionary dynamics

Muller plots represent subpopulation dynamics and phylogeny, while disregarding spatial information. The horizontal axis represents time and the vertical axis corresponds to subpopulation frequency. Each subpopulation is depicted as a shaded area emerging from its immediate ancestor (Figure 5b). Fish plots are similar but show population size rather than frequency (Figure 5c). Software packages for producing these plots include *ggmuller* [78] and *EvoFreq* [79].

### 6.3 Phenotype space plots

In a phenotype space plot, the axes correspond to continuous traits such as cell fitness, metabolic type, and degree of drug resistance, and each point represents a cell. We can visualize phenotypic evolution by animating phenotype space plots from a series of time points. Robertson-Tessi and colleagues pioneered the use of these plots in cancer research in their 2015 study of the effects of metabolic heterogeneity on tumour growth [48].

## 7 Reproducibility

Reproducibility is a cornerstone of the scientific method. A reproducible modelling study not only allows others to easily regenerate its results but also permits further data processing, downstream analysis of generated data, generation of summary statistics, ease of production for visual representations or plots, and even adaptation of the existing model for novel purposes.

### 7.1 Principles of reproducible research

Gundersen [80] describes three categories of reproducibility:

- Outcome reproducibility: The reproduction experiment's result matches the original. If the same analysis of the result is performed, the same conclusions can be drawn, and the original hypothesis is supported by both experiments.
- Analysis reproducibility: The reproduction experiment's result differs from the original, but if the same analysis method is used, the interpretation of the results still matches the original.
- Interpretation reproducibility: The reproduction experiment's outcomes and the analysis of said outcomes both differ, but the interpretation matches the original interpretation.

Computational modelling studies should typically aim for the highest standard of outcome reproducibility. If care is taken to construct a well-packaged computational study in a controlled digital environment, then in principle, given a suitable machine, the study should be easily reproduced exactly. This entails not only comprehensively explaining methods, results, analyses, and interpretation, but also sharing the model code and scripts used at every step of pre-processing and analysis, providing a detailed description of how to execute the code, and sharing any associated data and parameterisation and configuration files.

In their outline of best practices to observe throughout a computational research project, Sandve and colleagues [81] advocate tracking how every result is produced and reporting intermediate results as well as final outcomes. To make code easier to reproduce, one should catalogue the versions of software used at every point, record the seeds used in any random number generation, and implement version control [82]. Manual data manipulation should be avoided in favour of using automated methods to reformat and process raw data files. The raw data used to produce summary data plots should be easily accessible to facilitate easy plot reproduction and to allow readers to check individual data

1  
2  
3 467 points. Textual descriptions of methods and results should link to the associated raw data and code so that a reader can  
4 468 easily follow all the steps leading to interpretations. Lastly, modellers are highly encouraged to share each full study,  
5 469 ideally with a dedicated public server. One such research-oriented database is zenodo [83], where scientists may freely  
6 470 upload their research output permanently as a citeable piece of software.  
7  
8  
9

## 10 471 **7.2 Workflow managers, package managers and containers**

11  
12  
13 472 A complex computational model will often require multiple steps to be carried out in sequence. If a high-performance  
14 473 computing (HPC) cluster is required to run the model efficiently – as is typical for complex models – it is essential to  
15 474 utilise a workflow manager to properly orchestrate the steps [84]. Open-source workflow managers allow researchers  
16 475 to package a model into a reproducible, cross-platform workflow. Nextflow [85] and Snakemake [86] are among the  
17 476 most popular workflow managers with several published pipelines [87, 88, 89, 90], strong community support, and  
18 477 extensive documentation, giving users flexibility when designing their own custom pipelines. Snakemake is based  
19 478 on Python, a popular language among computational biologists and bioinformaticians. Nextflow uses the Java-based  
20 479 language Groovy, which has a Python-style structure and is relatively easy to for Python users to learn. Both also  
21 480 enable automatic parallelisation for HPC clusters, which can be essential for complex SABMs or for running multiple  
22 481 instances of smaller models simultaneously.  
23  
24  
25  
26  
27

28 482 Another option is to utilise container technologies, considered by many to be the gold standard in computational re-  
29 483 search. These are less computationally demanding than running an application on a computer directly or using a virtual  
30 484 machine and so permit faster deployment, patching, and scaling. Containers also allow users to deploy the application  
31 485 on multiple operating systems or machines without reformatting, and will run the application the same way no matter  
32 486 where they are deployed [91]. Docker [92] is a popular container design platform which permits packaging applica-  
33 487 tions into distribution-independent containers. Another option, Bioconda [93], enables easy dependency management,  
34 488 and can be deployed inside a container.  
35  
36  
37  
38  
39

## 40 489 **7.3 Extendable modelling platforms**

41  
42  
43 490 For many research projects, the easiest option can be to build on an existing open-source agent-based modelling  
44 491 platform (see appendix for a brief guide). Some of these platforms – such as Chaste [94], CompuCell3D [95], HAL  
45 492 [51] and PhysiCell [77] – excel in simulating off-lattice cell populations in complex microenvironments. Others, such  
46 493 as demon [96] (which has an automated computational workflow, Warlock [14]), J-SPACE [97] and SMITH [98],  
47 494 focus on efficient modelling of evolutionary dynamics. Several are modular platforms, which facilitate reproducibility  
48 495 by making it easy to create and share extensions of the generic software. Nevertheless, even the most flexible platform  
49 496 is necessarily based on certain fundamental assumptions, structures, and algorithms. If we want to create an especially  
50 497 innovative model, requiring several novel components that pre-existing modelling platforms lack, then we might find  
51 498 it best to start from scratch. In principle, specialist rather than generalist models permit greater optimisation in terms  
52 499 of memory demands and execution time.  
53  
54  
55  
56  
57  
58  
59  
60



#### 7.4 FAIR principles in data management

As the volume of publicly available research data has been growing exponentially in recent decades [99], proper digital data management and annotation is recognized as an essential step in computational research – crucial for research reproducibility. Most notably, the FAIR principles have become a cornerstone in modern data management, particularly in the realms of scientific and research data [100]. FAIR is an acronym that encapsulates a set of guiding principles: Findable, Accessible, Interoperable, and Reusable. To be FAIR, data must first be Findable, meaning that it is easy for both humans and machines to discover, thanks to comprehensive metadata and proper indexing. Data should be Accessible, ensuring that access rights and permissions are clear and well-defined, thus minimizing barriers to entry. Interoperable data is structured in a way that allows integration with other datasets by adhering to common standards, formats, and vocabularies. Lastly, data should be Reusable, with thorough documentation, contextual information, and availability in a format that facilitates easy replication and reuse. Altogether, the FAIR principles serve as a framework for enhancing data sharing, management, and collaboration, ultimately driving scientific progress and fostering open science initiatives. Major organisations that have embraced FAIR guidelines include the European Open Science Cloud [101], the European Life-Science Infrastructure for Biological Information [102], the US National Institutes of Health, and the Global Alliance for Genomics and Health [103].

#### Discussion

Having surveyed the numerous choices that arise in any SABM project, we are faced with a problem: how can we choose the most appropriate model? In tumour evolution research, unlike in much of physics and engineering, there is no standard approach. Rather we must tailor a model to each research question by considering which components, events and interactions must be included, how far each aspect can be parameterised with available data, and the limits of our computational resources. It is essential to build on a sound understanding of the biological system and of the questions that matter to biologists and clinicians. Ideally this knowledge should come through close collaboration with empirical researchers throughout the model development process.

A general principle is that model complexity should match the complexity only of the phenomena of interest. We need not employ an off-lattice hybrid SABM if a simple cellular automaton with only a few basic update rules can demonstrate the same principle. Attempting to represent every component of a biological system is not only computationally impractical but also risks overfitting and hinders explainability. Simpler models have many merits. They are easier to falsify and have fewer sources of potential error. They reduce researcher degrees of freedom and curb the tweaking of parameters to support a pet hypothesis. They are more mathematically tractable and easier to analyse. Perhaps most importantly, a simple model has wider applicability and can be more readily generalised, adapted or extended to answer new questions. More complicated models should be preferred only if the biological system is especially well understood or if simpler models have been tested and shown to be inadequate.

532 The greater difficulty – all too easily overlooked – is in choosing among a multitude of plausible simple models.  
533 An Eden growth model, for example, is arguably no more parsimonious than a spatial branching process or a spatial  
534 Moran process, which generate very different evolutionary dynamics. It is debatable whether the greater popularity of  
535 Eden growth models can be justified on biological grounds and is not simply due to them being easier to program.

536 Model design remains a challenge for even the most experienced researchers. One of the nine overarching themes in  
537 a recent review of key questions concerning the ecology and evolution of cancer [104] was that we do not yet know  
538 which mathematical and computational models are the most useful. In another recent survey of cancer adaptive therapy  
539 modelling [105], four of the eleven key open questions were related to identifying appropriate mathematical models.  
540 When it comes to SABMs, the main limitations are twofold. First, we typically lack sufficient data to design and  
541 parameterise SABMs of large tumours. Second, routinely simulating much more than a few million individual cells  
542 (corresponding to no more than half a cubic centimetre of tumour) is computationally impractical. To some extent,  
543 these problems have technological solutions. Multi-region sequencing, spatial multi-omics, digital pathology, and  
544 other modern methods are producing ever more detailed spatial tumour data. Accessible computing power continues  
545 to grow. But progress will also depend on developing smarter models.

546 Instead of drawing conclusions from a single SABM, we might do better to consider ensembles of models with diverse  
547 structures, algorithms, and underlying assumptions. Much as in hurricane forecasting [106], we can be more confident  
548 when many models converge on the same prediction. Another important direction is to develop coarse-grained models  
549 that can simulate tumour evolution as accurately as cell-level SABMs but with much greater computational efficiency.  
550 Rather than cell division, death, mutation and dispersal rates, coarse-grained models depend on macroscopic param-  
551 eters such as the arrival rate of consequential clones, clonal expansion speeds, and large-scale microenvironmental  
552 heterogeneity. A potential way forward is to combine mathematical analysis of the relevant stochastic processes to  
553 determine appropriate approximations [107], and machine learning methods to infer the parameter values. SABMs  
554 capable of accurately simulating the evolution of entire tumours could have wide-ranging applications, not least in  
555 patient-specific clinical forecasting.

## 556 References

- 557 [1] Matias Casás-Selves and James DeGregori. How cancer shapes evolution and how evolution shapes cancer.  
558 *Evolution: Education and outreach*, 4:624–634, 2011.
- 559 [2] Lauren MF Merlo, John W Pepper, Brian J Reid, and Carlo C Maley. Cancer as an evolutionary and ecological  
560 process. *Nature reviews cancer*, 6(12):924–935, 2006.
- 561 [3] Jing Yang, Tong-Jun Zhao, Chang-Qing Yuan, Jing-Hui Xie, and Fang-Fang Hao. A nonlinear competitive  
562 model of the prostate tumor growth under intermittent androgen suppression. *Journal of theoretical biology*,  
563 404:66–72, 2016.



A seven-step guide to spatial, agent-based modelling of tumour evolution

---

- 1  
2  
3 564 [4] David Basanta, Jacob G Scott, Russ Rockne, Kristin R Swanson, and Alexander RA Anderson. The role  
4 of *idh1* mutated tumour cells in secondary glioblastomas: an evolutionary game theoretical view. *Physical*  
5 565 *biology*, 8(1):015016, 2011.  
6 566  
7  
8 567 [5] Kaveh Danesh, Rick Durrett, Laura J Havrilesky, and Evan Myers. A branching process model of ovarian  
9 cancer. *Journal of theoretical biology*, 314:10–15, 2012.  
10 568  
11  
12 569 [6] Rick Durrett, Jasmine Foo, Kevin Leder, John Mayberry, and Franziska Michor. Evolutionary dynamics of  
13 tumor progression with random fitness values. *Theoretical population biology*, 78(1):54–66, 2010.  
14 570  
15 571 [7] Jeffrey West, Zaki Hasnain, Paul Macklin, and Paul K Newton. An evolutionary model of tumor cell kinetics  
16 and the emergence of molecular heterogeneity driving gompertzian growth. *SIAM review*, 58(4):716–736, 2016.  
17 572  
18  
19 573 [8] Richard Durrett, Jasmine Foo, and Kevin Leder. Spatial moran models, ii: cancer initiation in spatially struc-  
20 574 tured tissue. *Journal of mathematical biology*, 72:1369–1400, 2016.  
21  
22 575 [9] Serhii Aif, Nico Appold, Lucas Kampman, Oskar Hallatschek, and Jona Kayser. Evolutionary rescue of resistant  
23 mutants is governed by a balance between radial expansion and selection in compact populations. *Nature*  
24 576 *Communications*, 13(1):7916, 2022.  
25 577  
26  
27 578 [10] Daniel K Saha, Alexander RA Anderson, Luis Cisneros, and Carlo C Maley. In silico investigations of adaptive  
28 therapy using a single cytotoxic or a single cytostatic drug. *bioRxiv*, pages 2023–05, 2023.  
29 579  
30  
31 580 [11] Joshua A Bull and Helen M Byrne. Quantification of spatial and phenotypic heterogeneity in an agent-based  
32 581 model of tumour-macrophage interactions. *PLOS Computational Biology*, 19(3):e1010994, 2023.  
33  
34 582 [12] Robert Noble, Dominik Burri, Cécile Le Sueur, Jeanne Lemant, Yannick Viossat, Jakob Nikolas Kather, and  
35 Niko Beerenwinkel. Spatial structure governs the mode of tumour evolution. *Nature ecology & evolution*,  
36 583 6(2):207–217, 2022.  
37 584  
38  
39 585 [13] Robert Noble, John T Burley, Cécile Le Sueur, and Michael E Hochberg. When, why and how tumour clonal  
40 diversity predicts survival. *Evolutionary applications*, 13(7):1558–1568, 2020.  
41 586  
42  
43 587 [14] Maciej Bak, Blair Colyer, Veselin Manojlović, and Robert Noble. Warlock: an automated computational work-  
44 588 flow for simulating spatially structured tumour evolution. *arXiv preprint arXiv:2301.07808*, 2023.  
45  
46 589 [15] Katarina Bacevic, Robert Noble, Ahmed Soffar, Orchid Wael Ammar, Benjamin Boszonyik, Susana Prieto,  
47 Charles Vincent, Michael E Hochberg, Liliana Krasinska, and Daniel Fisher. Spatial competition constrains  
48 590 resistance to targeted cancer therapy. *Nature communications*, 8(1):1995, 2017.  
49 591  
50  
51 592 [16] Maximilian AR Strobl, Jill Gallaher, Jeffrey West, Mark Robertson-Tessi, Philip K Maini, and Alexander RA  
52 Anderson. Spatial structure impacts adaptive therapy by shaping intra-tumoral competition. *Communications*  
53 593 *medicine*, 2(1):46, 2022.  
54 594  
55  
56 595 [17] Joel L Schiff. *Cellular automata: a discrete view of the world*. John Wiley & Sons, 2011.  
57  
58  
59  
60

## A seven-step guide to spatial, agent-based modelling of tumour evolution

- 1  
2  
3  
4 596 [18] Pierre-Yves Louis and Francesca R Nardi. Probabilistic cellular automata. *Emergence, Complexity, Computa-*  
5 597 *tion*, 27, 2018.
- 6  
7 598 [19] Murray Eden. A two-dimensional growth process. *Dynamics of fractal surfaces*, 4:223–239, 1961.
- 8  
9 599 [20] R Jullien and R Botet. Scaling properties of the surface of the eden model in  $d= 2, 3, 4$ . *Journal of Physics A:*  
10 600 *Mathematical and general*, 18(12):2279, 1985.
- 11  
12 601 [21] Haider Tari, Ketty Kessler, Nick Trahearn, Benjamin Werner, Maria Vinci, Chris Jones, and Andrea Sottoriva.  
13 602 Quantification of spatial subclonal interactions enhancing the invasive phenotype of pediatric glioma. *Cell*  
14 603 *Reports*, 40(9), 2022.
- 15  
16  
17 604 [22] Sara Hamis, James Yates, Mark AJ Chaplain, and Gibin G Powathil. Targeting cellular dna damage responses  
18 605 in cancer: an in vitro-calibrated agent-based model simulating monolayer and spheroid treatment responses to  
19 606 atr-inhibiting drugs. *Bulletin of Mathematical Biology*, 83:1–21, 2021.
- 20  
21  
22 607 [23] Bartlomiej Waclaw, Ivana Bozic, Meredith E Pittman, Ralph H Hruban, Bert Vogelstein, and Martin A  
23 608 Nowak. A spatial model predicts that dispersal and cell turnover limit intratumour heterogeneity. *Nature*,  
24 609 525(7568):261–264, 2015.
- 25  
26  
27 610 [24] Maya A. Lewinsohn, Trevor Bedford, Nicola F. Müller, and Alison F. Feder. State-dependent evolutionary  
28 611 models reveal modes of solid tumour growth. *Nature Ecology & Evolution*, 7(4):581–596, 2023.
- 29  
30  
31 612 [25] Xiao Fu, Yue Zhao, Jose I. Lopez, Andrew Rowan, Lewis Au, Annika Fendler, Steve Hazell, Hang Xu, Stu-  
32 613 art Horswell, Scott T. C. Shepherd, Charlotte E. Spencer, Lavinia Spain, Fiona Byrne, Gordon Stamp, Tim  
33 614 O’Brien, David Nicol, Marcellus Augustine, Ashish Chandra, Sarah Rudman, Antonia Toncheva, Andrew J. S.  
34 615 Furness, Lisa Pickering, Santosh Kumar, Dow-Mu Koh, Christina Messiou, Derfel ap Dafydd, Matthew R.  
35 616 Orton, Simon J. Doran, James Larkin, Charles Swanton, Erik Sahai, Kevin Litchfield, Samra Turajlic, Ben  
36 617 Challacombe, Simon Chowdhury, William Drake, Archana Fernando, Nicos Fotiadis, Emine Hatipoglu, Karen  
37 618 Harrison-Phipps, Peter Hill, Catherine Horsfield, Teresa Marafioti, Jonathon Olsburgh, Alexander Polson, Ser-  
38 619 gio Quezada, Mary Varia, Hema Verma, Paul A. Bates, and on behalf of the TRACERx Renal Consortium.  
39 620 Spatial patterns of tumour growth impact clonal diversification in a computational model and the tracerx renal  
40 621 study. *Nature Ecology & Evolution*, 6(1):88–102, 2022.
- 41  
42  
43 622 [26] Nick Jagiella, Benedikt Müller, Margareta Müller, Irene E Vignon-Clementel, and Dirk Drasdo. Inferring  
44 623 growth control mechanisms in growing multi-cellular spheroids of nslc cells from spatial-temporal image  
45 624 data. *PLoS computational biology*, 12(2):e1004412, 2016.
- 46  
47  
48 625 [27] Ketevan Chkhaidze, Timon Heide, Benjamin Werner, Marc J Williams, Weini Huang, Giulio Caravagna,  
49 626 Trevor A Graham, and Andrea Sottoriva. Spatially constrained tumour growth affects the patterns of clonal  
50 627 selection and neutral drift in cancer genomic data. *PLoS computational biology*, 15(7):e1007243, 2019.
- 51  
52  
53 628 [28] Richard Durrett. Random graph dynamics, 2007.

A seven-step guide to spatial, agent-based modelling of tumour evolution

---

- 1  
2  
3 629 [29] Trevor Williams and Rolf Bjerknes. Stochastic model for abnormal clone spread through epithelial basal layer.  
4 630 *Nature*, 236(5340):19–21, 1972.
- 6 631 [30] François Graner and James A Glazier. Simulation of biological cell sorting using a two-dimensional extended  
7 632 potts model. *Physical review letters*, 69(13):2013, 1992.
- 10 633 [31] Nicholas J Savill and Paulien Hogeweg. Modelling morphogenesis: from single cells to crawling slugs. *Journal*  
11 634 *of theoretical biology*, 184(3):229–235, 1997.
- 13 635 [32] András Szabó and Roeland MH Merks. Cellular potts modeling of tumor growth, tumor invasion, and tumor  
14 636 evolution. *Frontiers in oncology*, 3:87, 2013.
- 17 637 [33] Jonathan F Li and John Lowengrub. The effects of cell compressibility, motility and contact inhibition on the  
18 638 growth of tumor cell clusters using the cellular potts model. *Journal of theoretical biology*, 343:79–91, 2014.
- 20 639 [34] Andreas Deutsch and Sabine Dormann. *Mathematical modeling of biological pattern formation*. Springer,  
21 640 2005.
- 24 641 [35] Andreas Deutsch, Josué Manik Nava-Sedeño, Simon Syga, and Haralampos Hatzikirou. Bio-Igca: a cellular au-  
25 642 tomaton modelling class for analysing collective cell migration. *PLoS computational biology*, 17(6):e1009066,  
26 643 2021.
- 29 644 [36] Pahini Pandya, Jose L Orgaz, and Victoria Sanz-Moreno. Modes of invasion during tumour dissemination.  
30 645 *Molecular oncology*, 11(1):5–27, 2017.
- 32 646 [37] Alessandro Lugli, Inti Zlobec, Martin D Berger, Richard Kirsch, and Iris D Nagtegaal. Tumour budding in solid  
33 647 cancers. *Nature Reviews Clinical Oncology*, 18(2):101–115, 2021.
- 36 648 [38] Sean L Preston, Wai-Man Wong, Annie On-On Chan, Richard Poulson, Rosemary Jeffery, Robert A Good-  
37 649 lad, Nikki Mandir, George Elia, Marco Novelli, Walter F Bodmer, et al. Bottom-up histogenesis of colorec-  
38 650 tal adenomas: origin in the monocryptal adenoma and initial expansion by crypt fission. *Cancer research*,  
39 651 63(13):3819–3825, 2003.
- 42 652 [39] Patrick Alfred Pierce Moran. *Random processes in genetics*, 1958.
- 44 653 [40] Andrea Sottoriva, Haeyoun Kang, Zhicheng Ma, Trevor A Graham, Matthew P Salomon, Junsong Zhao, Paul  
45 654 Marjoram, Kimberly Siegmund, Michael F Press, Darryl Shibata, et al. A big bang model of human colorectal  
46 655 tumor growth. *Nature genetics*, 47(3):209–216, 2015.
- 49 656 [41] Kimberly D Siegmund, Paul Marjoram, Yen-Jung Woo, Simon Tavaré, and Darryl Shibata. Inferring clonal  
50 657 expansion and cancer stem cell dynamics from dna methylation patterns in colorectal cancers. *Proceedings of*  
51 658 *the National Academy of Sciences*, 106(12):4828–4833, 2009.
- 54 659 [42] Niko Beerenwinkel, Roland F Schwarz, Moritz Gerstung, and Florian Markowetz. Cancer evolution: mathe-  
55 660 matical models and computational inference. *Systematic biology*, 64(1):e1–e25, 2015.

## A seven-step guide to spatial, agent-based modelling of tumour evolution

- 1  
2  
3  
4 661 [43] Benjamin Franz, Chuan Xue, Kevin J Painter, and Radek Erban. Travelling waves in hybrid chemotaxis models.  
5 662 *Bulletin of mathematical biology*, 76:377–400, 2014.
- 6  
7 663 [44] Paul Macklin, Mary E Edgerton, Alastair M Thompson, and Vittorio Cristini. Patient-calibrated agent-based  
8 664 modelling of ductal carcinoma in situ (dcis): from microscopic measurements to macroscopic predictions of  
9 665 clinical progression. *Journal of theoretical biology*, 301:122–140, 2012.
- 10  
11  
12 666 [45] Philip Gerlee and Alexander RA Anderson. Modelling evolutionary cell behaviour using neural networks:  
13 667 application to tumour growth. *Biosystems*, 95(2):166–174, 2009.
- 14  
15 668 [46] Jill A Gallaher, Pedro M Enriquez-Navas, Kimberly A Luddy, Robert A Gatenby, and Alexander RA Anderson.  
16 669 Spatial heterogeneity and evolutionary dynamics modulate time to recurrence in continuous and adaptive cancer  
17 670 therapies. *Cancer research*, 78(8):2127–2139, 2018.
- 18  
19  
20 671 [47] Keith S Hoek, Ossia M Eichhoff, Natalie C Schlegel, Udo Döbbeling, Nikita Kobert, Leo Schaerer, Silvio  
21 672 Hemmi, and Reinhard Dummer. In vivo switching of human melanoma cells between proliferative and invasive  
22 673 states. *Cancer research*, 68(3):650–656, 2008.
- 23  
24  
25 674 [48] Mark Robertson-Tessi, Robert J Gillies, Robert A Gatenby, and Alexander RA Anderson. Impact of metabolic  
26 675 heterogeneity on tumor growth, invasion, and treatment outcomes. *Cancer research*, 75(8):1567–1579, 2015.
- 27  
28  
29 676 [49] Motoo Kimura. The number of heterozygous nucleotide sites maintained in a finite population due to steady  
30 677 flux of mutations. *Genetics*, 61(4):893, 1969.
- 31  
32  
33 678 [50] Ryan O Schenck, Eunjung Kim, Rafael R Bravo, Jeffrey West, Simon Leedham, Darryl Shibata, and Alexan-  
34 679 der RA Anderson. Homeostasis limits keratinocyte evolution. *Proceedings of the National Academy of Sciences*,  
35 680 119(35):e2006487119, 2022.
- 36  
37 681 [51] Jeffrey West. Hybrid automata library. <https://halloworld.org>.
- 38  
39 682 [52] Robert Noble. An eden model in r (with optional mutation of division rates). [https://github.com/](https://github.com/robjohnnoble/EdenModel)  
40 683 [robjohnnoble/EdenModel](https://github.com/robjohnnoble/EdenModel), 2018.
- 41  
42  
43 684 [53] Daniel T Gillespie. A general method for numerically simulating the stochastic time evolution of coupled  
44 685 chemical reactions. *Journal of computational physics*, 22(4):403–434, 1976.
- 45  
46 686 [54] Daniel T Gillespie. Approximate accelerated stochastic simulation of chemically reacting systems. *The Journal*  
47 687 *of chemical physics*, 115(4):1716–1733, 2001.
- 48  
49  
50 688 [55] Takayuki Osogami and Mor Harchol-Balter. Closed form solutions for mapping general distributions to quasi-  
51 689 minimal ph distributions. *Performance Evaluation*, 63(6):524–552, 2006.
- 52  
53 690 [56] Giulia Belluccini, Martín López-García, Grant Lythe, and Carmen Molina-París. Counting generations in birth  
54 691 and death processes with competing erlang and exponential waiting times. *Scientific Reports*, 12(1):11289,  
55 692 2022.

## A seven-step guide to spatial, agent-based modelling of tumour evolution

- 1  
2  
3 [57] Nicole M Anderson and M Celeste Simon. The tumor microenvironment. *Current Biology*, 30(16):R921–R925,  
4 693 2020.  
5 694
- 6 [58] MA Chaplain and AR Anderson. Mathematical modelling, simulation and prediction of tumour-induced angio-  
7 695 genesis. *Invasion & metastasis*, 16(4-5):222–234, 1996.  
8 696
- 9 [59] An-Shen Qi, Xiang Zheng, Chan-Ying Du, and Bao-Sheng An. A cellular automaton model of cancerous  
10 697 growth. *Journal of theoretical biology*, 161(1):1–12, 1993.  
11 698
- 12 [60] Aalpen A Patel, Edward T Gawlinski, Susan K Lemieux, and Robert A Gatenby. A cellular automaton model  
13 699 of early tumor growth and invasion: the effects of native tissue vascularity and increased anaerobic tumor  
14 700 metabolism. *Journal of theoretical biology*, 213(3):315–331, 2001.  
15 701
- 16 [61] William H Press. *Numerical recipes 3rd edition: The art of scientific computing*. Cambridge university press,  
17 702 2007.  
18 703
- 19 [62] Ahmadreza Ghaffarizadeh, Samuel H Friedman, and Paul Macklin. Biofvm: an efficient, parallelized diffusive  
20 704 transport solver for 3-d biological simulations. *Bioinformatics*, 32(8):1256–1258, 2016.  
21 705
- 22 [63] Rafael R Bravo, Etienne Baratchart, Jeffrey West, Ryan O Schenck, Anna K Miller, Jill Gallaher, Chan-  
23 706 dler D Gatenbee, David Basanta, Mark Robertson-Tessi, and Alexander RA Anderson. Hybrid automata li-  
24 707 brary: A flexible platform for hybrid modeling with real-time visualization. *PLoS computational biology*,  
25 708 16(3):e1007635, 2020.  
26 709
- 27 [64] Joseph J Casciari, Stratis V Sotirchos, and Robert M Sutherland. Mathematical modelling of microenvironment  
28 710 and growth in emt6/ro multicellular tumour spheroids. *Cell proliferation*, 25(1):1–22, 1992.  
29 711
- 30 [65] Yangjin Kim, Magdalena A Stolarska, and Hans G Othmer. A hybrid model for tumor spheroid growth in  
31 712 vitro i: theoretical development and early results. *Mathematical Models and Methods in Applied Sciences*,  
32 713 17(supp01):1773–1798, 2007.  
33 714
- 34 [66] David Robert Grimes, Catherine Kelly, Katarzyna Bloch, and Mike Partridge. A method for estimating  
35 715 the oxygen consumption rate in multicellular tumour spheroids. *Journal of The Royal Society Interface*,  
36 716 11(92):20131124, 2014.  
37 717
- 38 [67] Joseph J Casciari, Stratis V Sotirchos, and Robert M Sutherland. Variations in tumor cell growth rates and  
39 718 metabolism with oxygen concentration, glucose concentration, and extracellular ph. *Journal of cellular physi-*  
40 719 *ology*, 151(2):386–394, 1992.  
41 720
- 42 [68] David Robert Grimes, Alexander G Fletcher, and Mike Partridge. Oxygen consumption dynamics in steady-  
43 721 state tumour models. *Royal Society open science*, 1(1):140080, 2014.  
44 722
- 45 [69] Arturo Araujo and David Basanta. Hybrid discrete-continuum cellular automaton (hca) model of prostate to  
46 723 bone metastasis. *bioRxiv*, page 043620, 2016.  
47 724

## A seven-step guide to spatial, agent-based modelling of tumour evolution

- [70] Arturo Araujo, Leah M Cook, Conor C Lynch, and David Basanta. Size matters: Metastatic cluster size and stromal recruitment in the establishment of successful prostate cancer to bone metastases. *Bulletin of mathematical biology*, 80:1046–1058, 2018.
- [71] Arturo Araujo, Leah M Cook, Conor C Lynch, and David Basanta. An integrated computational model of the bone microenvironment in bone-metastatic prostate cancer. *Cancer research*, 74(9):2391–2401, 2014.
- [72] Andrea Sottoriva and Simon Tavaré. Integrating approximate bayesian computation with complex agent-based models for cancer research. In *Proceedings of COMPSTAT'2010: 19th International Conference on Computational Statistics Paris France, August 22-27, 2010 Keynote, Invited and Contributed Papers*, pages 57–66. Springer, 2010.
- [73] Colin G Cess and Stacey D Finley. Calibrating agent-based models to tumor images using representation learning. *PLOS Computational Biology*, 19(4):e1011070, 2023.
- [74] Il'ya Meerovich Sobol'. On the distribution of points in a cube and the approximate evaluation of integrals. *Zhurnal Vychislitel'noi Matematiki i Matematicheskoi Fiziki*, 7(4):784–802, 1967.
- [75] Michael D McKay, Richard J Beckman, and William J Conover. A comparison of three methods for selecting values of input variables in the analysis of output from a computer code. *Technometrics*, 42(1):55–61, 2000.
- [76] Sara Hamis, Stanislav Stratiev, and Gibin G Powathil. Uncertainty and sensitivity analyses methods for agent-based mathematical models: An introductory review. *The Physics of Cancer: Research Advances*, pages 1–37, 2021.
- [77] Ahmadreza Ghaffarizadeh, Randy Heiland, Samuel H Friedman, Shannon M Mumenthaler, and Paul Macklin. Physicell: An open source physics-based cell simulator for 3-d multicellular systems. *PLoS computational biology*, 14(2):e1005991, 2018.
- [78] Robert Noble. ggmuller: Create muller plots of evolutionary dynamics. r package version 0.5.3. <https://CRAN.R-project.org/package=ggmuller>, 2019.
- [79] Chandler D Gatenbee, Ryan O Schenck, Rafael R Bravo, and Alexander RA Anderson. Evofreq: visualization of the evolutionary frequencies of sequence and model data. *BMC bioinformatics*, 20:1–4, 2019.
- [80] Odd Erik Gundersen. The fundamental principles of reproducibility. *Philosophical Transactions of the Royal Society A*, 379(2197):20200210, 2021.
- [81] Geir Kjetil Sandve, Anton Nekrutenko, James Taylor, and Eivind Hovig. Ten simple rules for reproducible computational research. *PLoS computational biology*, 9(10):e1003285, 2013.
- [82] Michael A Heroux and James M Willenbring. Barely sufficient software engineering: 10 practices to improve your cse software. In *2009 ICSE workshop on software engineering for computational science and engineering*, pages 15–21. IEEE, 2009.
- [83] Zenodo. <https://zenodo.org/>, 2023.

## A seven-step guide to spatial, agent-based modelling of tumour evolution

- 1  
2  
3 758 [84] Laura Wratten, Andreas Wilm, and Jonathan Göke. Reproducible, scalable, and shareable analysis pipelines  
4 with bioinformatics workflow managers. *Nature methods*, 18(10):1161–1168, 2021.  
5 759
- 6 760 [85] Felix Mölder, Kim Philipp Jablonski, Brice Letcher, Michael B Hall, Christopher H Tomkins-Tinch, Vanessa  
7 Sochat, Jan Forster, Soohyun Lee, Sven O Twardziok, Alexander Kanitz, et al. Sustainable data analysis with  
8 snakemake. *F1000Research*, 10, 2021.  
9 761  
10 762
- 11 763 [86] Paolo Di Tommaso, Maria Chatzou, Evan W Floden, Pablo Prieto Barja, Emilio Palumbo, and Cedric  
12 Notredame. Nextflow enables reproducible computational workflows. *Nature biotechnology*, 35(4):316–319,  
13 2017.  
14 764  
15 765
- 16 766 [87] Silas Kieser, Joseph Brown, Evgeny M Zdobnov, Mirko Trajkovski, and Lee Ann McCue. Atlas: a snakemake  
17 workflow for assembly, annotation, and genomic binning of metagenome sequence data. *BMC bioinformatics*,  
18 21:1–8, 2020.  
19 767  
20 768
- 21 769 [88] Martin Hölzer and Manja Marz. Poseidon: a nextflow pipeline for the detection of evolutionary recombination  
22 events and positive selection. *Bioinformatics*, 37(7):1018–1020, 2021.  
23 770  
24
- 25 771 [89] Qi Zhao, Yu Sun, Dawei Wang, Hongwan Zhang, Kai Yu, Jian Zheng, and Zhixiang Zuo. Lncpipe: A nextflow-  
26 based pipeline for identification and analysis of long non-coding rnas from rna-seq data. *J Genet Genomics*,  
27 45(7):399–401, 2018.  
28 772  
29 773
- 30 774 [90] MacIntosh Cornwell, Mahesh Vangala, Len Taing, Zachary Herbert, Johannes Köster, Bo Li, Hanfei Sun,  
31 Taiwen Li, Jian Zhang, Xintao Qiu, et al. Viper: Visualization pipeline for rna-seq, a snakemake workflow for  
32 efficient and complete rna-seq analysis. *BMC bioinformatics*, 19:1–14, 2018.  
33 775  
34 776
- 35 777 [91] David Moreau, Kristina Wiebels, and Carl Boettiger. Containers for computational reproducibility. *Nature*  
36 *Reviews Methods Primers*, 3(1):50, 2023.  
37 778
- 38 779 [92] Dirk Merkel et al. Docker: lightweight linux containers for consistent development and deployment. *Linux j*,  
39 239(2):2, 2014.  
40 780
- 41 781 [93] Björn Grüning, Ryan Dale, Andreas Sjödin, Brad A Chapman, Jillian Rowe, Christopher H Tomkins-Tinch,  
42 Renan Valieris, Johannes Köster, and Bioconda Team. Bioconda: sustainable and comprehensive software  
43 distribution for the life sciences. *Nature methods*, 15(7):475–476, 2018.  
44 782  
45 783
- 46 784 [94] Gary R Mirams, Christopher J Arthurs, Miguel O Bernabeu, Rafel Bordas, Jonathan Cooper, Alberto Corrias,  
47 Yohan Davit, Sara-Jane Dunn, Alexander G Fletcher, Daniel G Harvey, et al. Chaste: an open source c++  
48 library for computational physiology and biology. *PLoS computational biology*, 9(3):e1002970, 2013.  
49 785  
50 786
- 51 787 [95] Maciej H Swat, Gilberto L Thomas, Julio M Belmonte, Abbas Shirinifard, Dimitrij Hmeljak, and James A  
52 Glazier. Multi-scale modeling of tissues using compucell3d. In *Methods in cell biology*, volume 110, pages  
53 325–366. Elsevier, 2012.  
54 788  
55 789
- 56 790 [96] Robert Noble. demon. [https://github.com/robjohnnoble/demon\\_model](https://github.com/robjohnnoble/demon_model), 2019.  
57  
58  
59  
60

A seven-step guide to spatial, agent-based modelling of tumour evolution

---

- 1  
2  
3  
4 791 [97] Fabrizio Angaroni, Alessandro Guidi, Gianluca Ascolani, Alberto d’Onofrio, Marco Antoniotti, and Alex Grauzdenzi. J-space: a julia package for the simulation of spatial models of cancer evolution and of sequencing  
5 792 denzi. *J-space: a julia package for the simulation of spatial models of cancer evolution and of sequencing*  
6 793 experiments. *BMC bioinformatics*, 23(1):269, 2022.
- 7  
8 794 [98] Adam Streck, Tom L Kaufmann, and Roland F Schwarz. Smith: spatially constrained stochastic model for  
9 795 simulation of intra-tumour heterogeneity. *Bioinformatics*, 39(3):btad102, 2023.
- 10  
11 796 [99] Volume of data/information created, captured, copied, and consumed worldwide from 2010 to 2020, with fore-  
12 797 casts from 2021 to 2025. <https://www.statista.com/statistics/871513/worldwide-data-created/>, August 2023.
- 13  
14  
15 798 [100] Mark D Wilkinson, Michel Dumontier, IJsbrand Jan Aalbersberg, Gabrielle Appleton, Myles Axton, Arie Baak,  
16 799 Niklas Blomberg, Jan-Willem Boiten, Luiz Bonino da Silva Santos, Philip E Bourne, et al. The fair guiding  
17 principles for scientific data management and stewardship. *Scientific data*, 3(1):1–9, 2016.
- 18 800
- 19  
20 801 [101] The european open science cloud (eosc). <https://eosc-portal.eu/about/eosc>.
- 21  
22 802 [102] European life-science infrastructure for biological information. <https://elixir-europe.org>.
- 23  
24 803 [103] Global alliance for genomics and health. <https://www.ga4gh.org>.
- 25  
26 804 [104] Antoine M Dujon, Athena Aktipis, Catherine Alix-Panabières, Sarah R Amend, Amy M Boddy, Joel S Brown,  
27 805 Jean-Pascal Capp, James DeGregori, Paul Ewald, Robert Gatenby, et al. Identifying key questions in the ecology  
28 806 and evolution of cancer. *Evolutionary Applications*, 14(4):877–892, 2021.
- 29  
30 807 [105] Jeffrey West, Fred Adler, Jill Gallaher, Maximilian Strobl, Renee Brady-Nicholls, Joel Brown, Mark Roberson-  
31 808 Tessi, Eunjung Kim, Robert Noble, Yannick Viossat, et al. A survey of open questions in adaptive therapy:  
32 809 Bridging mathematics and clinical translation. *Elife*, 12:e84263, 2023.
- 33  
34  
35 810 [106] Thomas M Hamill, Michael J Brennan, Barbara Brown, Mark DeMaria, Edward N Rappaport, and Zoltan Toth.  
36 811 Noaa’s future ensemble-based hurricane forecast products. *Bulletin of the American Meteorological Society*,  
37 812 93(2):209–220, 2012.
- 38  
39  
40 813 [107] Alexander Stein, Ramanarayanan Kizhuttill, Maciej Bak, and Robert Noble. The ubiquity of clonal interference  
41 814 in cancer and other range expansions. *bioRxiv*, 2024.

**Data archiving statement**

815  
816 Data sharing is not applicable to this article as no new data were created or analyzed in this study.